Cell Death and Differentiation (2017) 24, 2077–2088
 1350-9047/17

www.nature.com/cdd

Oxidative stress-induced S100B accumulation converts myoblasts into brown adipocytes via an NF-κB/YY1/miR-133 axis and NF-κB/YY1/BMP-7 axis

Giulio Morozzi[1,4], Sara Beccafico[1,2,4], Roberta Bianchi[1], Francesca Riuzzi[1,2], Ilaria Bellezza[1], Ileana Giambanco[1], Cataldo Arcuri[1], Alba Minelli[1] and Rosario Donato*[,1,2,3]

Muscles of sarcopenic people show hypotrophic myofibers and infiltration with adipose and, at later stages, fibrotic tissue. The origin of infiltrating adipocytes resides in fibro-adipogenic precursors and nonmyogenic mesenchymal progenitor cells, and in satellite cells, the adult stem cells of skeletal muscles. Myoblasts and brown adipocytes share a common *Myf5*$^+$ progenitor cell: the cell fate depends on levels of bone morphogenetic protein 7 (BMP-7), a TGF-β family member. S100B, a Ca^{2+}-binding protein of the EF-hand type, is expressed at relatively high levels in myoblasts from sarcopenic humans and exerts anti-myogenic effects via NF-κB-dependent inhibition of MyoD, a myogenic transcription factor acting upstream of the essential myogenic factor, myogenin. Adipogenesis requires high levels of ROS, and myoblasts of sarcopenic subjects show elevated ROS levels. Here we show that: (1) ROS overproduction in myoblasts results in upregulation of S100B levels via NF-κB activation; and (2) ROS/NF-κB-induced accumulation of S100B causes myoblast transition into brown adipocytes. S100B activates an NF-κB/Ying Yang 1 axis that negatively regulates the promyogenic and anti-adipogenic miR-133 with resultant accumulation of the brown adipogenic transcription regulator, PRDM-16. S100B also upregulates BMP-7 via NF-κB/Ying Yang 1 with resultant BMP-7 autocrine activity. Interestingly, myoblasts from sarcopenic humans show features of brown adipocytes. We also show that S100B levels and NF-κB activity are elevated in brown adipocytes obtained by culturing myoblasts in adipocyte differentiation medium and that S100B knockdown or NF-κB inhibition in myoblast-derived brown adipocytes reconverts them into fusion-competent myoblasts. At last, interstitial cells and, unexpectedly, a subpopulation of myofibers in muscles of geriatric but not young mice co-express S100B and the brown adipocyte marker, uncoupling protein-1. These results suggest that S100B is an important intracellular molecular signal regulating *Myf5*$^+$ progenitor cell differentiation into fusion-competent myoblasts or brown adipocytes depending on its levels.
Cell Death and Differentiation (2017) **24,** 2077–2088; doi:10.1038/cdd.2017.132; published online 8 September 2017

Sarcopenia manifests as reduced skeletal muscle mass and strength, increased fatigability and risk of bone fractures.[1,2] Sarcopenia is characteristic of aged (≥75-years old) people and represents a major health problem and an important burden for health systems because of the growing lifespan in advanced countries. Histologically, sarcopenic muscles show hypotrophic myofibers (mostly type II myofibers) and infiltration with adipose and, at later stages, fibrotic tissue and decreased numbers of satellite cells (SCs),[3] the adult stem cells of skeletal muscles located between the sarcolemma and the basal lamina.[4] SCs are essential for the maintenance of muscle mass.[4] Sarcopenia may be either secondary to chronic inflammatory statuses, diabetes, hormonal alterations, vascular disturbances and immobilization,[2] or primary, occurring in otherwise healthy, usually aged persons.[1] The pathogenesis of primary sarcopenia is not completely understood. Extrinsic, niche-related factors and intrinsic, cell-autonomous factors concur to determine changes in SCs, ultimately leading to reduced SCs' ability to maintain muscle mass.[4–11] Accumulation of reactive oxygen species (ROS) characterizes activated, aged SCs/proliferating aged myoblasts; possibly, ROS overproduction, owing to either altered mitochondrial function or defective ROS management, is one main cause of sarcopenia.[12,13] ROS overproduction might determine the aberrant p38 MAPK activity, deregulated p16 (INK4a) expression and JAK-STAT signaling and defective autophagy detected in aged SCs and suggested to be responsible for their altered proliferation and differentiation properties.[7–11]

Fat accumulation is observed in denervated muscle and atrophic muscle of elderly people.[14,15] The origin of infiltrating adipocytes resides in fibro-adipogenic precursors,[16–18] nonmyogenic mesenchymal progenitor cells[19] and SCs themselves.[19–22] Notably, ROS accumulation characterizes adipogenesis,[23] and oxidative stress induces adipogenic differentiation of skeletal myofiber-associated cells.[24]

Myoblasts and adipocytes share a common progenitor cell. Physiologically, mesenchimal stem cells differentiate into *Myf5*$^+$ myogenic lineage progenitors under the action of bone morphogenetic protein 7 (BMP-7), a TGF-β family member.[25]

[1]Department of Experimental Medicine, Istituto Interuniversitario di Miologia, Perugia Medical School, University of Perugia, Perugia, Italy; [2]Istituto Interuniversitario di Miologia, Perugia, Italy and [3]Centro Universitario per la Ricerca sulla Genomica Funzionale, Piazza Lucio Severi 1, Perugia 06132, Italy

*Corresponding author: R Donato, Department of Experimental Medicine, Perugia Medical School, University of Perugia, Piazza Lucio Severi 1, Perugia 06132, Italy. Tel: +39 75 5 858 256; E-mail: rosario.donato@unipg.it

[4]These authors contributed equally to this work.

Received 27.1.17; revised 20.6.17; accepted 03.7.17; Edited by JP Medema; published online 08.9.17

Myf5$^+$ progenitors can generate myoblasts and brown adipocytes,[26] and PAX7-expressing cells, that is SCs and their immediate progeny (i.e., proliferating myoblasts), can generate both brown adipocytes and skeletal muscle.[27] Cell fate decision depends on levels of BMP-7. Persisting BMP-7 causes *Myf5*$^+$ progenitors to differentiate into brown adipocytes by repressing the expression of the adipogenic inhibitors, Necdin (*Ndn)* and preadipocyte factor 1 (*Pref1)* and inducing the key molecular determinant, PRD1-BF1-RIZ1 homologous domain-containing 16 (PRDM-16).[28,29] In turn, PRDM-16 triggers the activation of the complete brown adipogenesis program and blocks the induction of myoblast-specific genes such as *Myf5* and *Myod1*. In the presence of low or no BMP-7 *Myf5*$^+$ progenitors proceed along the myogenic lineage by increasing *Myod1* expression levels.[25]

S100B protein is a Ca^{2+}-binding protein of the EF-hand type[30] expressed in mature myofibers, SCs, proliferating myoblasts and differentiated myocytes.[31] S100B associates with microtubules and type III intermediate filaments and negatively regulates their assembly state in a Ca^{2+}-dependent manner,[32,33] which might be important during cell division and myocyte fusion. S100B was shown to modulate myoblast differentiation by activating the IKKβ/NF-κB pathway, upregulating Yin Yang 1 (YY1), and inhibiting the expression of MyoD, a muscle-specific transcription factor responsible for the induction of the essential myogenic transcription factor, myogenin.[31] Upon transfer from growth medium (GM) to differentiation medium (DM), myoblasts transiently downregulate S100B expression in a p38 MAPK- and proteasome-dependent manner; S100B downregulation at the beginning of the myogenic differentiation process is permissive for myogenesis.[34,35] Interestingly, myoblasts derived from aged human SCs, which are proliferation and differentiation defective, show upregulated S100B levels, and knockdown of S100B partly reverts aged human myoblasts to a young phenotype.[34] Thus, elevated S100B levels contribute, at least in part, to the characteristically low myogenic potential of aged myoblasts.

In the present work we sought to investigate the relationship between chronic oxidative stress and S100B levels in myoblasts, and consequences of upregulation of S100B in terms of cell lineage identity. We found that (1) chronic oxidative stress is a potent inducer of S100B expression via NF-κB activation; (2) upregulated S100B causes myoblasts to convert into brown adipocytes via an NF-κB/YY1 axis that negatively regulates the promyogenic and anti-adipogenic miR-133 with consequent accumulation of the pro-brown adipogenic transcription regulator, PRDM-16, and an NF-κB/YY1/BMP-7 axis with resultant BMP-7 autocrine activity; (3) S100B levels are elevated in brown adipocytes obtained by culturing myoblasts in adipocyte differentiation medium (ADM) and S100B knockdown in myoblast-derived brown adipocytes reconverts them into fusion-competent myoblasts; and (4) muscles of geriatric but not young mice show expression of the brown adipocyte marker, uncoupling protein 1 (UCP-1) in interstitial cells and a subpopulation of myofibers, and uncoupling protein 1 (UCP-1) co-localizes with S100B at these sites.

Results

Chronic elevation of ROS levels inhibits myogenic differentiation and increases S100B levels. Paraquat (PQ) is a herbicide known to cause cell dysfunction via mitochondrial damage and ROS overproduction.[36] Treatment of C2C12 myoblasts for 72 h in GM with increasing PQ doses caused dose-dependent ROS production and reduction of cell viability at $\geq 100\,\mu$M (Figure 1a). Subsequent experiments with PQ were performed in the presence of 100 μM PQ because at this concentration PQ caused at 72 h a ~36% increase in ROS levels and a moderate (~29%) decrease in the cell number as a result of a ~48% increase in the percentage of cells in the sub-G1 phase of the cell cycle (essentially apoptotic cells), ~12% decrease in the percentage of cells in G0/G1 phase, ~30% decrease in the percentage of cells in S phase and ~100% increase in the percentage of cells in G2/M phase compared with controls (Figure 1a). Based on these results, in experiments performed in the presence of PQ, myoblasts were seeded at a 100% higher number in GM compared with the control to obtain comparable myoblast densities at 72 h.

Consistent with previous work,[37] chronic (72 h) treatment of C2C12 myoblasts with PQ in GM and DM caused a robust inhibition of myogenic differentiation. Specifically, PQ treatment reduced the number and size of myotubes (Figure 1b), and levels of phosphorylated (activated) p38 MAPK (the master kinase in the myogenic differentiation process), MyoD (a muscle-specific transcription factor required for myoblast proliferation arrest and capable of inducing myogenin), myogenin (an early myogenic differentiation marker essential for myogenic differentiation) and myosin heavy chain, a late myogenic differentiation marker[38] (Figure 1c). PQ treatment of myoblasts for 72 h in GM only was sufficient to significantly inhibit p38 MAPK and myogenic differentiation (Supplementary Figure S1a,b). The reduced p38 MAPK phosphorylation extent in PQ-treated myoblasts was likely dependent on ROS-dependent induction of the phosphatase, MKP-1 (*Dusp1*)[39] (Figure 1d). Also, PQ treatment of myoblasts in GM only resulted in enhanced NF-κB(p65) phosphorylation (activation) levels (Supplementary Figure S1b) as previously reported,[40] and in higher levels of S100B compared with controls (Supplementary Figure S1b). Similar levels of S100B were detected in PQ-treated and control myoblast cultures after 72 h in DM (Figure 1c). However, whereas in control cultures S100B was highly expressed in myotubes and myogenin$^+$ myocytes but not in non-differentiated (myogenin$^-$) myoblasts (Supplementary Figure S1c) as reported,[31,32] in PQ-treated cultures S100B was present in non-fused myogenin$^-$ myoblasts that represented the vast majority of the cells in this condition (Supplementary Figure S1c). Persistence of S100B in non-differentiated (myogenin$^-$), non-fused myoblasts in DM likely depended on the strongly reduced activation of p38 MAPK[31,32] consequent to chronic PQ treatment (Figure 1c and Supplementary Figure S1b) and/or other concurring events (see Figure 3a). Culturing myoblasts in the presence of the antioxidant, trolox (TLX), significantly reduced PQ-induced effects on ROS production (Supplementary Figure S2a), MyoD and S100B levels (Supplementary Figure S2b), and NF-κB(p65) transcriptional

activity (Supplementary Figure S2c). Thus, we tentatively ascribed the anti-myogenic effect of PQ to chronic ROS production and the enhanced activity of the anti-myogenic NF-κB(p65) and S100B.

Chronic oxidative conditions cause myoblast-brown adipocyte transition via upregulation of S100B. ROS accumulation characterizes adipogenesis.[23] As PQ-treated myoblasts in GM accumulated ROS (Figure 1a), showed high S100B levels (Supplementary Figure S1b) and low MyoD levels, and presented little or no expression of myogenic markers in DM (Figure 1c and Supplementary Figure S1c), we asked whether PQ and/or S100B might promote myoblast-adipocyte transition. PQ treatment of C2C12 myoblasts for 72 h in GM resulted in staining of $>90\%$ of cells with Oil Red O (ORO), that detects lipid droplets and marks adipocytes, with minimal ORO staining of control cells (Figures 2a and e). Similarly, the vast majority of myoblasts cultured for 72 h in DM following PQ treatment showed ORO staining compared with a few ORO-stained non-fused cells in control cultures (Figure 2a). Culturing myoblasts in the presence of TLX reduced PQ-induced effects on lipid droplet formation (Supplementary Figure S2d). Thus, PQ treatment might cause myoblast-adipocyte transition via ROS production.

We asked whether the elevated levels of S100B detected in PQ-treated myoblasts (Figure 1c and Supplementary Figure S1b,c) might have a role in myoblast-adipocyte transition. Transient transfection with bovine *S100b* (Figure 2b) resulted in ORO staining of $>70\%$ C2C12 myoblasts after 72 h in GM (Figure 2c). Also, L6C8 myoblasts, a clone of rat L6 myoblasts stably overexpressing S100B and incapable of differentiating into myocytes and of forming myotubes,[31] were nearly 100% ORO stained after 72 h in GM as opposed to essentially no ORO staining in control (L6C11) myoblasts (Figure 2d). Moreover, knockdown of S100B in PQ-treated C2C12 myoblasts resulted in little if any ORO staining (Figure 2e). Thus, S100B appears to be intrinsically endowed with proadipogenic properties in myoblasts and the proadipogenic effect of PQ in myoblasts might depend on S100B overexpression in part.

Next, we assessed in C2C12 myoblasts expression levels of factors known to regulate the commitment of *Myf5*$^+$ progenitors to myoblasts or brown adipocytes, including the peroxisome proliferator-activated receptor gamma (PPARγ) co-activator, *Prdm16*, a zinc-finger transcriptional regulator necessary and sufficient to establish the identity of the brown adipose tissue lineage,[26,28] and BMP-7 that, when released, induces *Prdm16* and PPARγ co-activator 1 α (*Pgc1a*) to increase the brown, but not white, adipose differentiation.[29] PQ-treated myoblasts in GM showed higher levels of *S100b*, the brown adipogenic factors, *Bmp7*, *Prdm16* and *Pgc1a*, and the brown adipocyte marker, *Ucp1*, lower levels of the anti-adipogenic factors *Pref1* and *Ndn*, and reduced levels of the myoblast-specific genes, *Pax7* and *Myod1* compared with controls (Figure 2f). Culturing myoblasts in the presence of TLX significantly reduced PQ-induced effects on *S100b*, BMP-7 (mRNA and protein), *Prdm16* and UCP-1 (mRNA and protein) levels (Supplementary Figure S2e). Thus, chronic oxidative conditions switched myoblasts towards a brown adipocyte phenotype. Transient transfection of C2C12 myoblasts with *S100b* also resulted in increased levels of *Prdm16*,

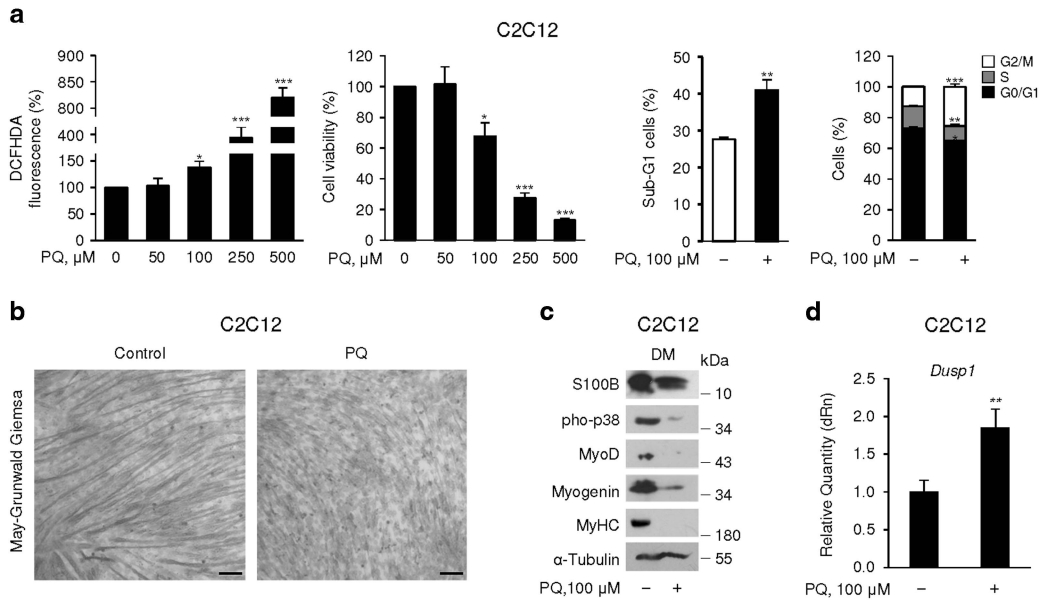

Figure 1 Chronic elevation of ROS levels inhibits myogenic differentiation and increases S100B levels. (**a**) C2C12 myoblasts were cultured in GM for 72 h in the presence of increasing doses of PQ. ROS production (left panel) and cell viability (middle panel) were measured and percentages of apoptotic (sub-G1) cells and cells in the G0/G1, S and G2/M phase of the cell cycle were calculated (right panels). (**b**) C2C12 myoblasts were cultured in GM for 72 h in the absence or presence of 100 μM PQ and then transferred to DM for another 72 h again in the absence or presence of 100 μM PQ. Cultures were subjected to May-Grunwald Giemsa staining. (**c**) Conditions were as in (**b**) except that cell lysates were subjected to western blotting for the detection of the indicated proteins. Tubulin was used as loading control. (**d**) Conditions were as in (**b**) except that cell lysates were analyzed by real-time PCR for detection of *Dusp1*. (b,**c**) One representative experiment of three. The mean percentages or fold changes ($\pm$S.E.M.) (N = 3) were determined (**a**, **d**). *, **, and *** significantly different from control ($P<0.05$, $P<0.01$ and $P<0.001$, respectively). Bar in (**b**) = 100 μm

Pgc1a, *Ucp1* and *Bmp7* and decreased levels of *Pref1*, *Pax7* and *Myod1* (Figure 2g) along with increased NF-κB(p65) phosphorylation levels and transcriptional activity and increased BMP-7 levels (Figure 2h), compared with controls. Similarly, L6C8 (S100B-overexpressing) myoblasts (Figure 2i, left panel) showed higher *Bmp7*, *Prdm16* and *Pgc1a* levels

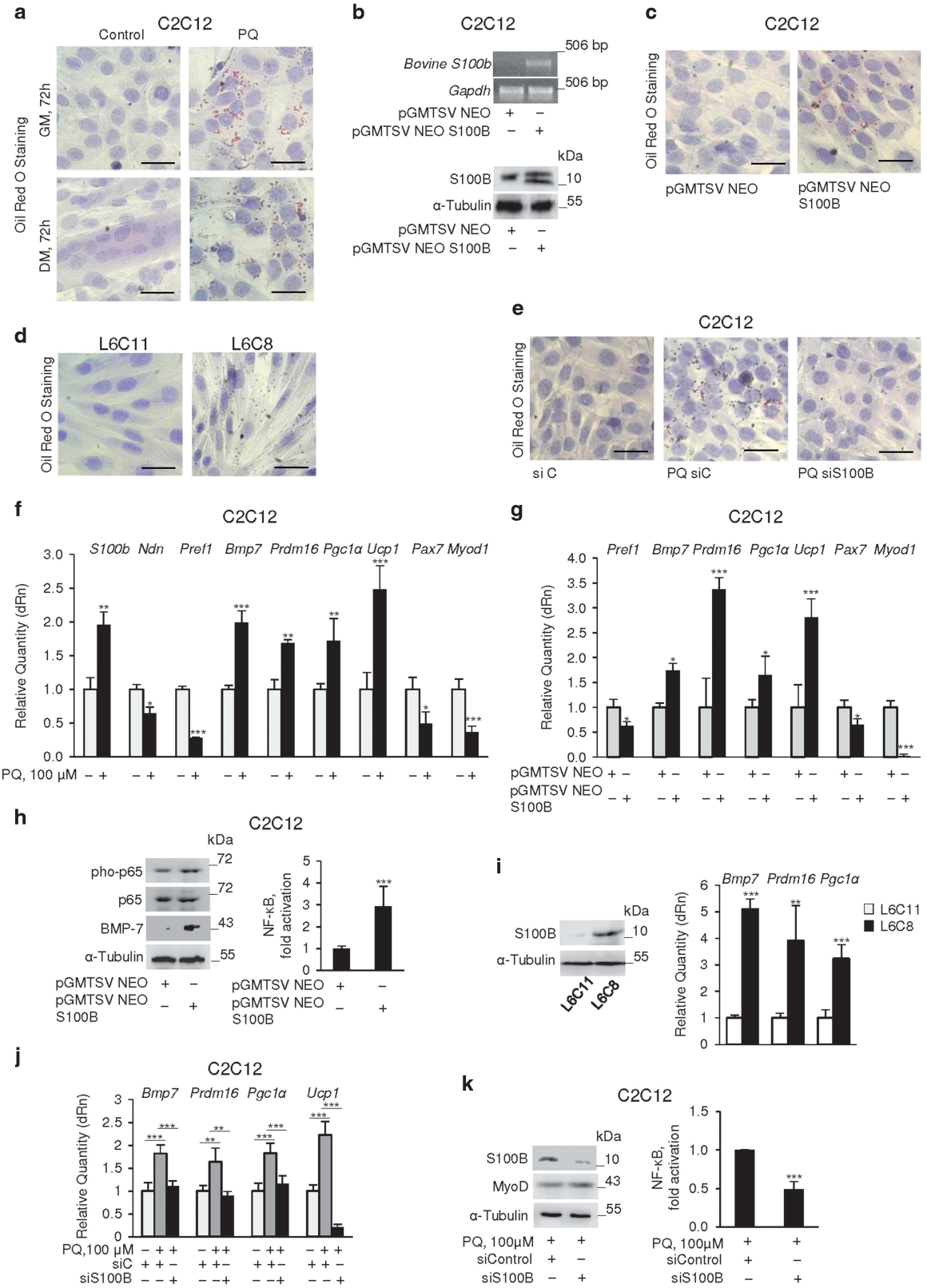

compared with L6C11 (mock-transfected) myoblasts (Figure 2i, right panel). Transient transfection of primary mouse myoblasts with bovine *S100b* led to increased levels of *Prdm16*, *Ucp1* and *Bmp7* (Supplementary Figure S3a) and size of lipid droplets (Supplementary Figure S3b) compared with controls. At last, knockdown of S100B in PQ-treated C2C12 myoblasts in GM reversed the PQ-induced increase in *Bmp7*, *Prdm16, Pgc1a* and *Ucp1* levels (Figure 2j) and PQ-induced increase in NF-κB transcriptional activity and decrease in MyoD levels (Figure 2k). Thus, at relatively high levels S100B might promote myoblast-brown adipocyte transition.

S100B and NF-κB(p65) regulate each other levels and YY1 levels. The anti-myogenic effect of intracellular S100B relies on its ability to stimulate NF-κB(p65) activity and NF-κB (p65)-dependent inhibition of MyoD expression[31] (also see Figures 2g,h and k). We found that S100B expression in C2C12 myoblasts is in turn positively regulated by NF-κB (p65). Indeed, inhibition of NF-κB(p65) activity by treatment of C2C12 myoblasts with the NF-κB(p65) inhibitor, sulfasalazine (SSN), reduced S100B mRNA and protein levels in control and PQ-treated myoblasts in GM (Figure 3a) in agreement with the presence of four NF-κB(p65) recognition sites in the *S100b* promoter (1000 bp upstream of the transcription initiation site) and NF-κB(p65)-dependent induction of S100B expression in other experimental settings.[41] Thus, a reciprocal regulation of S100B and NF-κB(p65) might occur in myoblasts whereby S100B stimulates NF-κB(p65) activity and NF-κB(p65) upregulates S100B.

Notably, either PQ treatment (Figure 3a) or *S100b* transfection (Figure 3b) of C2C12 myoblasts caused upregulation of mRNA and protein levels of YY1, a transcriptional repressor induced by NF-κB(p65) with anti-myogenic activity.[42] Inhibition of NF-κB (p65) reversed PQ effects on YY1 and BMP-7 mRNA and protein levels and *Pref1*, *Prdm16* and *Ucp1* levels (Figure 3a) and reduced lipid droplet formation in PQ-treated C2C12 myoblasts and untreated L6C8 myoblasts (Figure 3c). Treatment with TLX also reduced PQ-induced upregulation of YY1 (Supplementary Figure S2f). Further, L6C8 myoblasts showed higher *Yy1* levels compared with L6C11 myoblasts (Figure 3d) as reported,[31] and treatment of L6C8 myoblasts with SSN reduced *Yy1*, *Prdm16, Bmp7* and *Pgc1a* levels (Figure 3d). Lastly, treatment of L6C8 myoblasts with a specific YY1 siRNA inhibited lipid droplet formation (Figure 3e) and reduced *Bmp7* and *Prdm16* levels (Figure 3f). Thus, S100B, induced by NF-κB (p65), might activate NF-κB(p65) in myoblasts to increase its own levels and levels of the proadipogenic BMP-7, *Prdm16* and *Pgc1a*, of *Ucp1* and of the anti-myogenic and, as shown here for the first time, brown adipogenic YY1, and to decrease the anti-adipogenic *Pref1*.

S100B reduces levels of miR-133, a promyogenic and anti-adipogenic factor. The muscle-specific miRNA, miR-133, regulates myoblast proliferation and differentiation[43,44] and prevents myoblast-brown adipocyte transition by repressing *Prdm16* expression.[45,46] The observation that *Yy1* negatively regulates the expression of muscle-specific miRNAs including miR-133[47] and the finding that S100B upregulates YY1[31] (also see Figure 3b) prompted us to investigate potential interactions between S100B and miR-133 in the context of myoblast-brown adipocyte transition. Either PQ treatment (Figure 4a) or transient transfection with *S100b* (Figure 4b) caused down-regulation of miR-133 in C2C12 myoblasts in both GM and DM, and inhibition of NF-κB with SSN in PQ-treated C2C12 myoblasts restored miR-133 levels (Figure 4c). Thus, the pro-brown adipogenic effects of S100B and NF-κB might be mediated by repression of miR-133 likely via upregulation of YY1.

Chronic oxidative conditions and/or upregulation of S100B increase BMP-7 secretion with resultant autocrine pro-brown adipogenic effects of BMP-7. Culture media of C2C12 and L6C11 myoblasts in GM contained minimal if any BMP-7, whereas culture media of PQ-treated C2C12 myoblasts and L6C8 myoblasts contained large BMP-7 amounts (Figure 5a). Culturing PQ-treated C2C12 myoblasts in the presence of a BMP-7-neutralizing antibody caused a robust decrease in ORO staining compared with non-immune IgG-treated controls (Figure 5b) and reversed PQ effects on *S100b*, *Pref1*, *Yy1*, *Prdm16* and *Ucp1* levels (Figure 5c). Similarly, blocking extracellular BMP-7 in *S100b*-transfected C2C12 myoblasts reduced *Bmp7*, *Prdm16*, *Pgc1a* and *Ucp1* levels compared with the control (Figure 5d). Also, culturing L6C11 myoblasts in the presence of conditioned medium from L6C8 myoblasts caused lipid droplet formation (Figure 5e) and enhanced *Yy1*, *Bmp7*, *Prdm16* and *Pgc1a* levels (Figure 5f). Thus, PQ- and S100B-induced myoblast-brown adipocyte transition might also depend on induction and secretion of BMP-7 and autocrine BMP-7-dependent induction of *Bmp7* itself, *Yy1*, *Prdm16*, *Pgc1a* and *S100b*, and BMP-7 effects might be mediated by S100B in part.

Figure 2 Chronic oxidative conditions cause myoblast-brown adipocyte transition via upregulation of S100B. (**a**) C2C12 myoblasts were cultured in GM for 72 h in the absence or presence of 100 μM PQ and then transferred to DM for another 72 h in the absence or presence of 100 μM PQ. Cells were then stained with ORO. (**b**) C2C12 myoblasts were cultured in GM for 72 h and transfected with bovine *S100b*. Cells were analyzed for expression of *S100b* by RT-PCR (top panel) and of S100B by western blotting (bottom panel). Tubulin was used as loading control. (**c**) Conditions were as in (**b**) except that cells were subjected to ORO staining. (**d**) L6C11 (control) and L6C8 (S100B overexpressing) myoblasts were cultured in GM for 72 h and stained with ORO. (**e**) C2C12 myoblasts were cultured in GM for 72 h in the absence or presence of 100 μM PQ, transfected with S100B siRNA and stained with ORO. (**f**) C2C12 myoblasts were cultured in GM for 72 h in the absence or presence of 100 μM PQ and analyzed by real-time PCR. (**g**) Conditions were as in (**b** and **c**) except that cells were analyzed by real-time PCR. (**h**) Conditions were as in (**b**) except that cells were analyzed by western blotting (left panel) or transfected with NF-κB-luc reporter gene for measurement of NF-κB transcriptional activity (right panel). (**i**) L6C11 and L6C8 myoblasts were cultured in GM and analyzed for expression of S100B (left panel) and the indicated genes (right panel). (**j**) Conditions were as in e except that cells were analyzed for expression of the indicated genes. (**k**) Conditions were as in (**e**) except that cells were analyzed for S100B and MyoD levels and NF-κB transcriptional activity. (**a**–**e**) one representative experiment of three. The fold changes (±S.E.M.) ($N=3$) were determined (**f**, **g**, **j** and **h**, **i**, **k** right panels). *, ** and *** significantly different from control ($P<0.05$, $P<0.01$ and $P<0.001$, respectively). Bars in (**a**), (**c**–**e**) = 100 μm

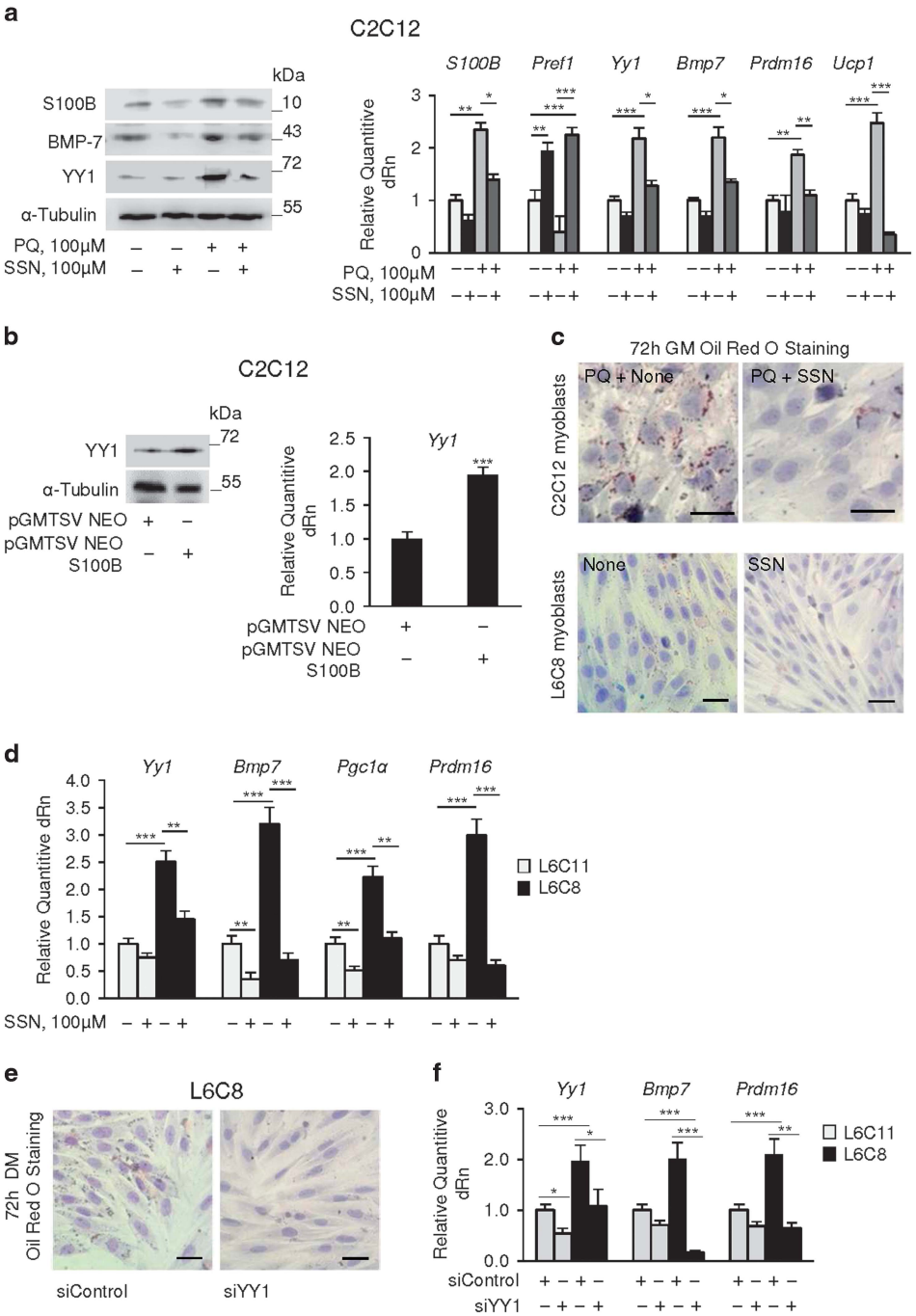

Figure 3 S100B and NF-κB(p65) regulate each other levels and levels of YY1. (**a**) C2C12 myoblasts were cultured in GM for 72 h in the absence or presence of 100 μM PQ ± sulfasalazine (SSN) and analyzed by western blotting (left panel) and real-time PCR (right panel). (**b**) C2C12 myoblasts were cultured in GM for 72 h, transfected with *S100b* and analyzed for levels of YY1 by western blotting and real-time PCR. (**c**) C2C12 myoblasts cultured in GM for 72 h in the presence of 100 μM PQ ± SSN and L6C8 myoblasts cultured in GM for 72 h ± SSN were stained with ORO. (**d**) L6C11 and L6C8 myoblasts were cultured in GM for 72 h and analyzed by real-time PCR. (**e**) L6C8 myoblasts were transfected with YY1 siRNA in GM, transferred to DM for 72 h and stained with ORO. (**f**) L6C11 and L6C8 myoblasts were transfected with YY1 siRNA in GM and analyzed by real-time PCR. (**a**, **b**) (left panels) (**c**, **e**): one representative experiment of three. The fold changes (± S.E.M.) ($N=3$) were determined (**a**, **b** right panels, **d**, **f**). *, ** and *** significantly different from control ($P<0.05$, $P<0.01$ and $P<0.001$, respectively). Bars in (**c**, **e**) = 100 μm

Myoblasts from aged sarcopenic humans show features of brown adipocytes. Myoblasts from sarcopenic humans are differentiation defective and show high levels of S100B and low p38 MAPK phosphorylation levels compared with myoblasts from non-sarcopenic subjects.[34] Myoblasts from aged sarcopenic but not young subjects showed ORO staining in both GM and DM (Figures 6a and b) and higher YY1 and BMP-7 levels compared with young subjects (Figure 6c). Thus, myoblasts from sarcopenic subjects resemble PQ-treated C2C12 myoblasts in terms of S100B,

YY1, and BMP-7 levels, p38 MAPK phosphorylation levels[34] and of lipid droplet formation, which is in agreement with the chronic oxidative conditions that characterize sarcopenic myoblasts.[48] Thus, chronic oxidative conditions might increase S100B levels, which in turn might promote myoblast-brown adipocyte transition in aged human myoblasts.

S100B becomes upregulated in an NF-κB-dependent manner in myoblasts cultured in ADM promoting myoblast-brown adipocyte transition, and co-localizes with UCP-1-expressing cells and myofibers in geriatric muscles. C2C12 myoblasts show features of pluripotent mesenchimal stem cells and exhibit myogenic, osteogenic and adipogenic differentiation markers.[20] When exposed to a cocktail of the phosphodiesterase inhibitor 3-isobutyl-1-methylxanthine, dexamethasone and insulin (ADM),[49] C2C12 myoblasts differentiate into adipocytes.[50] Culturing C2C12 myoblasts in ADM caused upregulation of S100B and UCP-1 (mRNA and protein), *Yy1*, *Bmp7* and *Prdm16* levels and enhancement of NF-κB transcriptional activity (Figure 7a) and formation of lipid droplets (Figure 7b). Inhibition of NF-κB with SSN or S100B knockdown robustly reduced ADM effects on *S100b*, *Ucp1*, *Yy1*, *Bmp7* and *Prdm16* levels and caused a ~75% and 50% reduction of ORO-stained cell numbers, respectively, with accompanying change of the cell shape from round to fusiform (Figures 7a and b). Thus, S100B and NF-κB appear to be important molecular determinants of ADM-induced C2C12 differentiation into brown adipocytes. Further, shifting cells from ADM to GM for 3 days resulted in no major changes compared with the ADM condition, however S100B knockdown caused myotube formation (Figure 7b). Thus, reducing S100B levels in myoblast-derived brown adipocytes was sufficient for reverting them to fusion-competent myoblasts even in GM. Likewise, switching primary mouse myoblasts to ADM led to increased *S100b*, *Ucp1*, *Yy1*, *Bmp7, Pgc1a*, *Prdm16*, S100B, BMP-7, YY1 and UCP-1 levels (Supplementary Figure S3c) along with increased ORO staining (Supplementary Figure S3d). Also, muscles of geriatric (28 months old) and young (2 months old) mice showed expression of S100B in a subpopulation of myofibers as expected[31] with higher levels in geriatric myofibers (Figures 7c and d). Notably however, geriatric but not young muscles showed co-expression of S100B and UCP-1 in interstitial cells and, unexpectedly, in the S100B$^+$ subpopulation of myofibers including thin, regenerating (i.e., centrally nucleated) myofibers (Figure 7c). Geriatric muscle tissue contained UCP-1 by western blot analysis as opposed to the almost complete absence of UCP-1 in young muscles (Figure 7d).

Discussion

Chronic oxidative conditions induce adipogenic differentiation of skeletal myofiber-associated cells,[24] and overproduction of ROS consequent to either altered mitochondrial function or defective ROS management, is considered characteristic of activated, aged SCs/proliferating aged myoblasts and hence one main cause of sarcopenia.[11–13] In the present report we have shown that chronic oxidative conditions cause myoblast-brown adipocyte transition via NF-κB(p65)-dependent upregulation of S100B and S100B-dependent activation of an NF-κB/YY1 axis, leading to downregulation of the promyogenic and anti-adipogenic myomiR, miR-133 and consequent[45,46] upregulation the essential brown adipogenic *Prdm16* (Figure 7e). The S100B/NF-κB(p65)/YY1 axis also upregulates the brown adipogenic BMP-7 and the resultant enhanced extracellular levels of BMP-7 upregulate *Bmp7* itself, *S100b* and *Prdm16* (Figure 7e). Notably, *Bmp7* expression was shown to be positively regulated by NF-κB (p65) in other experimental settings.[51] Moreover, culturing C2C12 myoblasts in ADM results in myoblast-brown adipocyte transition and enhanced NF-κB activity and S100B expression. ADM-induced upregulation of S100B plays an important role in this transition as S100B knockdown in myoblast-derived brown adipocytes causes their reversal to fusion-competent myoblasts. Interestingly, myoblasts derived from isolated aged hu-SCs show features of brown adipocytes, and primary mouse myoblasts behave essentially as do C2C12 myoblasts in terms of conversion to brown adipocytes when transfected with *S100b* or switched to ADM. Lastly, muscles of geriatric but not young mice co-express S100B and

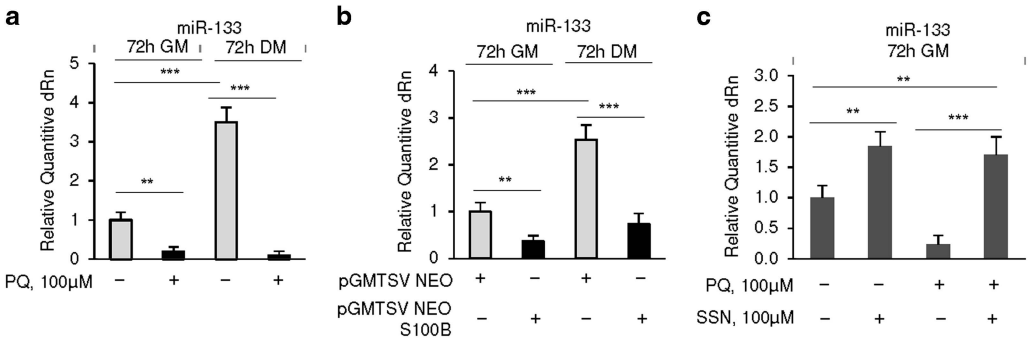

Figure 4 S100B reduces expression levels of miR-133, a promyogenic and anti-adipogenic factor. (**a**) C2C12 myoblasts were cultured in either GM or DM for 72 h in the absence or presence of 100 μM PQ and analyzed for levels of miR-133 by real-time PCR. (**b**) C2C12 myoblasts were cultured in GM for 72 h, transfected with *S100b* and either analyzed for levels of miR-133 by real-time PCR or transferred to DM for 72 h and analyzed for levels of miR-133 by real-time PCR. (**c**) C2C12 myoblasts were cultured in GM for 72 h in the absence or presence of 100 μM PQ ± SSN and analyzed for levels of miR-133 by real-time PCR. The fold changes (± S.E.M.) ($N=3$) were determined (**a–c**). *, ** and ***significantly different from control ($P<0.05$, $P<0.01$ and $P<0.001$, respectively)

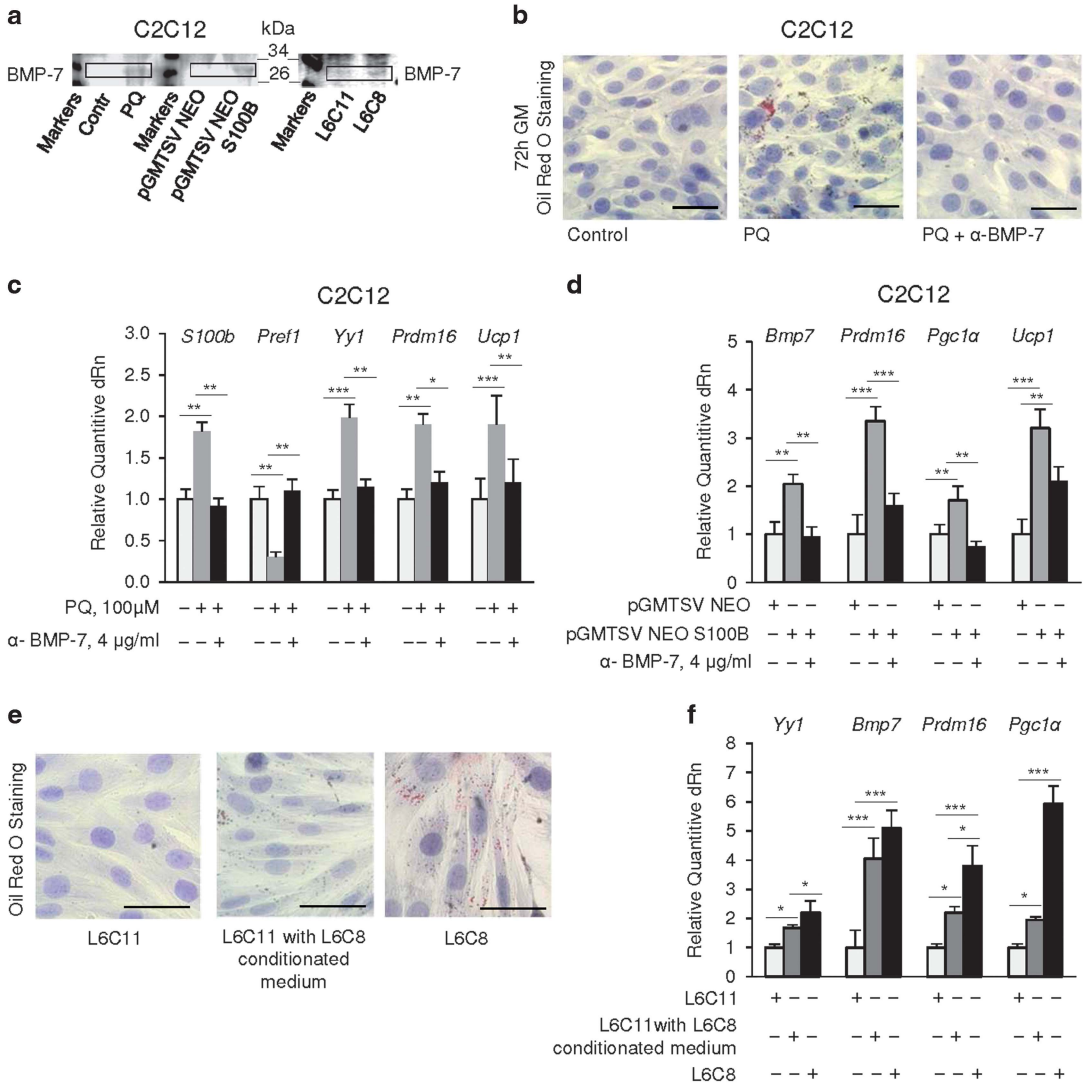

Figure 5 Chronic oxidative conditions and/or upregulation of S100B expression increase BMP-7 secretion and autocrine pro-brown adipogenic effects of BMP-7. (**a**) C2C12 myoblasts were cultured in GM for 72 h in the absence or presence of 100 μM PQ or transfected with *S100b*. Parallel L6C11 and L6C8 myoblasts were cultured in GM for 72 h. Culture media were collected, TCA precipitated and analyzed for expression of BMP-7 by western blotting. (**b**) C2C12 myoblasts were cultured in GM for 72 h in the absence or presence of 100 μM PQ $\pm$ non-immune IgG (control and PQ) or neutralizing anti-BMP-7 antibody (4 μg/ml). Cells were stained with ORO. (**c**) Conditions were as in **b** except that cells were analyzed by real-time PCR. (**d**) C2C12 myoblasts were transfected with *S100b* in GM and treated with non-immune IgG or neutralizing anti-BMP-7 antibody (4 μg/ml). Cells were analyzed by real-time PCR. (**e**) L6C11 myoblasts were cultured for 72 h in the absence (left panel) or presence (middle panel) of L6C8 conditioned medium and stained with ORO. Parallel L6C8 myoblasts (right panel) also were stained with ORO. (**f**) Conditions were as in (**e**) except that cells were analyzed by real-time PCR. (**a**,**b**,**e**): one representative experiment of three. The fold changes ($\pm$S.E.M.) ($N=3$) were determined (**c**, **d**, **f**). *, ** and ***significantly different from control ($P<0.05$, $P<0.01$ and $P<0.001$, respectively). Bars in (**b**, **e**) = 100 μm

the brown adipogenic marker, UCP-1, in interstitial cells as well as in a subpopulation of myofibers.

Previous work has shown that YY1 is required for mitochondrial morphology and bioenergetic function in skeletal muscle tissue[52] and recently, YY1 in brown adipose tissue has been shown to activate the canonical thermogenic and uncoupling gene expression program.[53] Our novel results suggest that YY1, induced by S100B via NF-κB in chronic oxidative conditions or under the autocrine action of BMP-7 in S100B-overexpressing myoblasts, promotes myoblast-brown adipocyte transition, which might have important implications in the pathophysiology of primary sarcopenia. In this regard, it is notable that myoblasts derived from aged sarcopenic humans show elevated levels of S100B and YY1, which might reduce their myogenic potential by driving their transition to brown adipocytes. Incidentally, we show that S100B/NF-κB-induced YY1 promotes myoblast-brown adipocyte transition as opposed to the inhibitory effects of YY1 on the transition of preadipocytes to white adipocytes.[54]

Both microenvironmental conditions[5,6] and cell intrinsic properties[7–11] are responsible for the reduced myogenic potential of myofiber-associated stem cells seen in sarcopenia. A reduced ability to manage ROS appears to be one major cause of muscle wasting in elderly people[11–13] and, possibly,

of the aforementioned alterations in aged SCs.[48] Our present results suggest that ROS/NF-κB-induced accumulation of S100B in aged SCs/myoblasts might represent an important piece of the complex molecular mosaic behind sarcopenia. Indeed, S100B-induced myoblast-brown adipocyte transition can be reversed by S100B knockdown. Thus, we propose that the anti-myogenic properties of intracellular S100B[31,34] might be exerted (1) via the known ability of NF-κB/YY1 to repress MyoD and myogenin expression[40,42] likely through NF-κB/YY1-induced reduction of expression of the promyogenic and anti-adipogenic myomiR, miR-133, with resultant upregulation of *Prdm16* levels, and (2) via NF-κB/YY1-mediated upregulation of BMP-7 and resultant BMP-7-dependent myoblast-brown adipocyte transition.

Fat accumulation is a major pathogenic factor in sarcopenia,[3] and S100B is found in high abundance in white adipocytes,[55] brown adipocytes, particularly paucilocular and unilocular brown adipocytes,[56] and in breast, cardiac and intraosseous hibernoma.[57–59] As shown here, in geriatric muscles S100B co-localizes with UCP-1$^+$ interstitial cells, i.e., *bona fide* brown adipocytes, and in a subpopulation of medium-sized myofibers and regenerating myofibers. Collectively, our results suggest that ROS/NF-κB-induced S100B might be a major molecular determinant of myoblast-brown adipocyte transition having an important role in the brown adipocyte-like features of myoblasts from sarcopenic humans and a potential therapeutic target. The previously unreported finding of UCP-1 expression within geriatric myofibers calls for an in-depth investigation of the functional role of UCP-1 and the S100B-UCP-1 interplay in these myofibers.

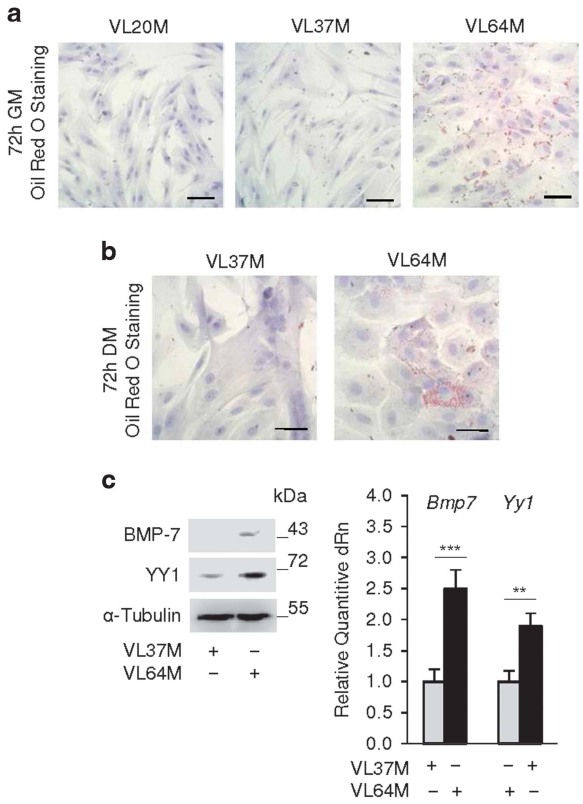

Figure 6 Myoblasts from aged sarcopenic humans show features of brown adipocytes. (**a**, **b**) Human myoblasts derived from SCs isolated from *Vastus lateralis* muscles of two young (20 years and 37-years old) males (VL20M and VL37M) and one sarcopenic male (VL64M) were cultured in GM for 72 h (**a**) and transferred to DM for 72 h (**b**) and stained with ORO. (**c**) VL37M and VL64M myoblasts were cultured in GM for 72 h and analyzed for expression of BMP-7 and YY1 by western blotting and real-time PCR. **a**, **c** and **c** left panel: one representative experiment of three. The fold changes ($\pm$S.E.M.) ($N=3$) were determined (c right panel). **, and *** significantly different from control ($P<0.01$ and $P<0.001$, respectively). Bars in (**a**, **b**) = 100 μm

Materials and Methods

Antibodies and oligonucleotide sequences. Antibodies and oligonucleotide sequences are listed in Supplementary Experimental Procedures (Supplementary Table S1 and Supplementary Table S2, respectively).

Cell culture. C2C12 and primary myoblasts were seeded in Dulbecco's modified Eagle medium (DMEM) (Invitrogen) supplemented with 20% FBS (Gibco Life Technologies, Milan, Italy), 100 U/ml penicillin and 100 mg/ml streptomycin (GM), in an H_2O-saturated 5% CO2 atmosphere at 37 °C and left undisturbed for 72 h. Where required, myoblasts were shifted either to DMEM supplemented with 2% horse serum (HS) (Euroclone, Milan, Italy), 100 U/ml penicillin, and 100 mg/ml streptomycin (DM) and cultured for 24–72 h, or to DMEM supplemented with 10% FBS, 100 U/ml penicillin, and 100 mg/ml streptomycin containing 0.5 mM phosphodiesterase inhibitor 3-isobutyl-1-methylxanthine, 1 μM dexamethasone and 850 nM/ml insulin (all from Sigma-Aldrich S.r.l., Milan, Italy) (ADM) and left undisturbed for 3 days. L6C11 and L6C8 rat myoblasts[31] were seeded in DMEM supplemented with 10% FBS and antibiotics as reported[31] and cultured for 72 h. Where required cells were treated with PQ (Sigma) in the absence or presence of either 100 μM SSN (Sigma-Aldrich S.r.l.) or 100 μM TLX (Sigma-Aldrich S.r.l.). Myoblast derived from human SCs were provided by the University of Chieti-Pescara, Italy, and were obtained from *Vastus lateralis* muscle biopsies of young and aged healthy untrained humans, following informed consent, enrolled in a study approved by the Ethics Committee for Biomedical Research of the University of Chieti-Pescara, Italy, (PROT 1884 COET) and complying with the Declaration of Helsinki (amended in 2000). Human myoblasts were grown in HAM's F-10 (Gibco Life Technologies) supplemented with 100 U/ml penicillin, 100 mg/ml streptomycin and 50 μg/ml gentamycin (GM), in an H_2O-saturated 5% CO2 atmosphere at 37 °C. To induce myogenic differentiation, human myoblasts were transferred to HG-DMEM supplemented with 2% HS, antibiotics as above, 10 μg/ml insulin and 100 μg/ml apotransferrin for 3 days.

ROS production, MTT and cell cycle analysis. The 2',7'-dichlorodihydrofluorescein diacetate (DCFH-DA) method was used to detect ROS intracellular levels by a conventional assay. The fluorescence of DCFH-DA was detected at 485nm excitation and at 535nm emission. Cell viability was assessed by the conventional MTT (3-[4,5-dimethylthiazol-2-yl]-2,5-dephenyl tetrazolium bromide) reduction assay. Results are expressed as the percentages of reduced MTT, assuming the absorbance of control cells as 100%. To measure apoptosis and analyze cell cycle, myoblasts were seeded onto 35-mm plastic dishes for 72 h in GM in the absence or presence of 100 μM PQ. The apoptotic cells suspended in the culture medium were collected, washed twice with PBS and resuspended in propidium iodide (PI) solution (0.1% sodium citrate, 0.1% Triton X-100 and 50 mg/l PI). Cell cycle progression also was analyzed by PI staining. In brief, adherent cells were washed twice in PBS and incubated for 30 min at 4 °C with PI solution. Percentages of apoptotic cells and cells in the various phases of the cell cycle were measured by flow cytometry using fluorescence-activated cell sorting (FACS, Coulter Epics XL-MLC).

May-Grunwald Giemsa and ORO staining and immunofluorescence. Cells were fixed for 7 min with cold methanol, washed three times with deionized water, dried in a heater and subjected to May-Grunwald Giemsa staining following a standard procedure. For ORO staining, cells were fixed with paraformaldehyde (Sigma-Aldrich S.r.l.) (4% in PBS) for 10 min at room temperature and stained either with ORO (Sigma-Aldrich S.r.l.). Cells were then washed 2–3 times with water and incubated for 2 min with Hematoxylin (Bioptica, Milan, Italy) and washed until the water was clear. The cells were viewed in a phase contrast microscope (Olympus IX51) equipped with a digital camera (Olympus C-5050 ZOOM), and the images were acquired at 20x magnification. For double immunofluorescence, the cells were fixed with 4% paraformaldehyde in PBS for

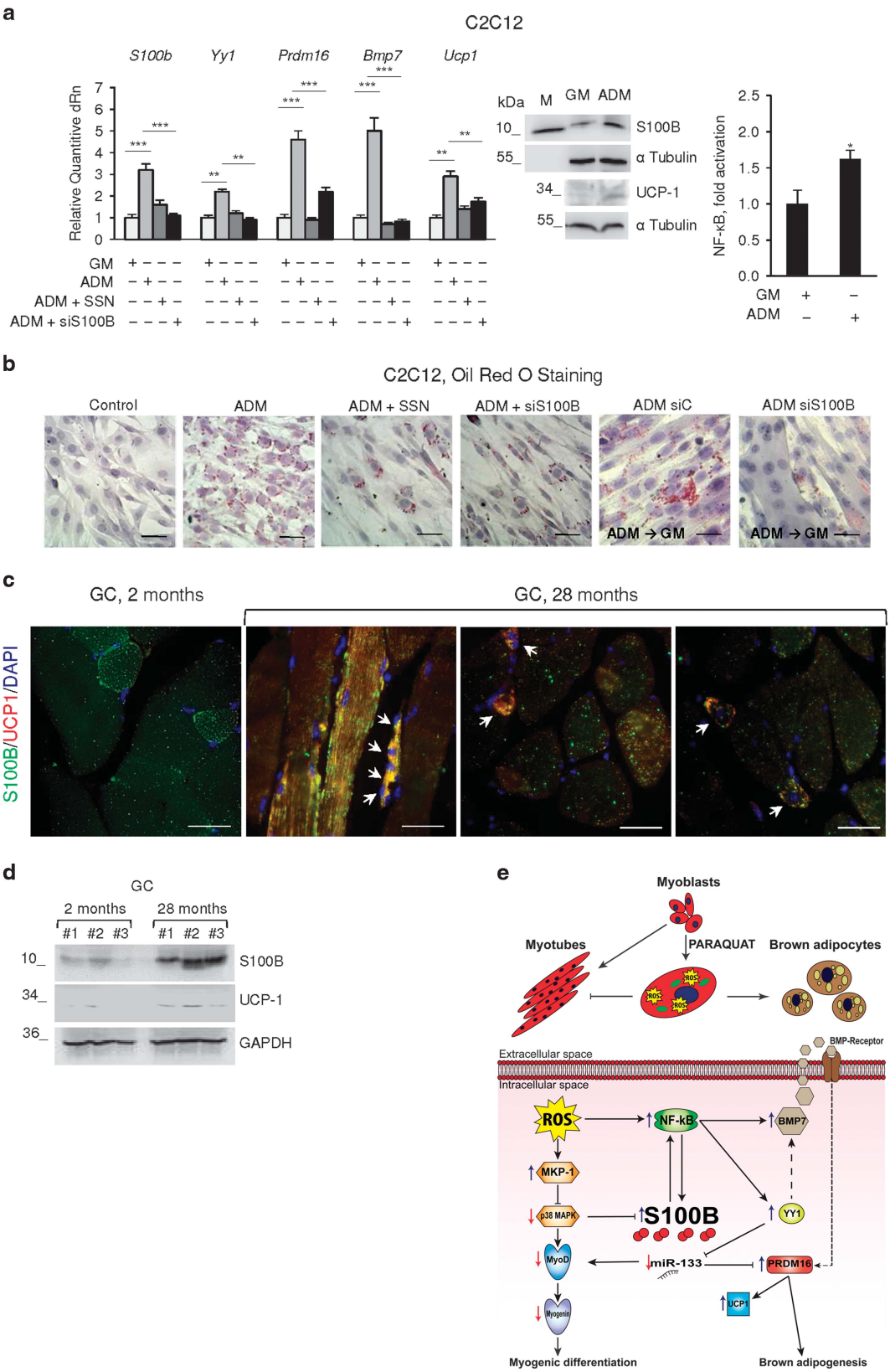
a
C2C12
S100b
Yy1
Prdm16
Bmp7
Ucp1
Relative Quantitive dRn
GM
ADM
ADM + SSN
ADM + siS100B
kDa M GM ADM
10_
S100B
55_
α Tubulin
34_
UCP-1
55_
α Tubulin
NF-κB, fold activation
b
C2C12, Oil Red O Staining
Control
ADM
ADM + SSN
ADM + siS100B
ADM siC
ADM siS100B
ADM → GM
ADM → GM
c
GC, 2 months
GC, 28 months
S100B/UCP1/DAPI
d
GC
2 months
28 months
#1 #2 #3
#1 #2 #3
10_
S100B
34_
UCP-1
36_
GAPDH
e
Myoblasts
Myotubes
PARAQUAT
Brown adipocytes
Extracellular space
Intracellular space
BMP-Receptor
ROS
NF-kB
BMP7
MKP-1
p38 MAPK
S100B
YY1
MyoD
miR-133
PRDM16
UCP1
Myogenin
Myogenic differentiation
Brown adipogenesis

Figure 7 S100B becomes upregulated in an NF-κB-dependent manner in myoblasts cultured in ADM and promotes myoblast-brown adipocyte transition. (**a**) Left panel: C2C12 myoblasts were cultivated in GM for 72 h and then transferred to ADM ± SSN for 3 days. Cells in ADM (3 days) were transfected with S100B siRNA and cultured for another 24 h. Cells were analyzed by real-time PCR. Middle panel: C2C12 myoblasts were cultured in GM and/or ADM and analyzed for S100B and UCP-1 expression by western blotting. Right panel: conditions were as for middle panel except that cells were analyzed for NF-κB transcriptional activity. (**b**) Conditions were as in (**a**, left panel) except that cells were ORO stained (top and middle panels). Parallel cells cultured in ADM were transfected with control siRNA (siC) or S100B siRNA, transferred to GM for 72 h and ORO stained (bottom panels). (**c, d**) *Gastrocnemius* (GC) muscles of young (2-month old) and geriatric (28-month old) mice were analyzed for S100B and UCP-1 expression by double immunofluorescence (**c**) and western blotting (**d**). Arrows in (**c**) point to double S100B$^+$-UCP-1$^+$ interstitial cells (left and middle panels) and to regenerating (centrally nucleated) myofibers (right panel) in geriatric muscles. (**a**) (middle panel), (**b–d**): one representative experiment of three. The fold changes (± S.E.M.) ($N = 3$) were determined (**a**, right and left panel). *significantly different from control ($P < 0.05$). Bars in (**a**, **b**) = 100 μm; in (**c**) = 50 μm. (**e**) Schematic representation of effects of chronic oxidative conditions in myoblasts. Chronic oxidative conditions generated by treatment with PQ, promote myoblast-brown adipocyte transition via ROS/NF-κB-dependent upregulation of S100B and ROS-induced upregulation of MKP-1, resulting in inhibition of the promyogenic p38 MAPK with consequent accumulation of S100B. S100B in turn, stimulates NF-κB transcriptional activity with resultant upregulation of YY1 and downregulation of the promyogenic and anti-adipogenic miR-133. Reduction of miR-133 levels causes the upregulation of PRDM-16 with resultant stimulation of brown adipogenesis. NF-κB also upregulates BMP-7 that acts in an autocrine/paracrine manner to promote myoblast-brown adipocyte transition. How YY1 regulates BMP-7 expression remains to be established (dashed arrow). The scheme does not take into account the role(s) of S100B and UCP-1 in muscles of geriatric mice

10 min at room temperature, washed three times in PBS, and sequentially incubated for 1 h at room temperature with 0.4% Triton X-100, 1% BSA and 10% HS in PBS (blocking buffer), and overnight in a humid chamber at 4 °C with a polyclonal anti-S100B antibody (1:20, Abcam, Cambridge, UK) in combination with a monoclonal anti-myogenin antibody (1:20, Santa Cruz Biotechnology, Heidelberg, Germany). After washed in 0–1% Tween-20 in PBS, the cells were incubated for l h at room temperature with Alexa fluor 594 donkey anti-mouse antibody and Alexa fluor 466 donkey anti-rabbit antibody (both 1:200, Invitrogen). Nuclei were counterstained with 4',6-diamnidino-2-phenylindole (DAPI). After rinsing, samples were mounted with fluorescent mounting medium (Dako Corporation, Carpinteria, Canada) and viewed in an epifluorescence microscope (Leica, Milan, Italy, DMRB) equipped with a digital camera.

Western blotting. Cells were homogenized in 50 mM Tris pH 7.4, 150 mM NaCl, 1% Triton X-100, in the presence of a mixture of protease inhibitors (Roche Applied Science, Milan, Italy). The amount of protein in each samples was determined by Bradford assay and equal amounts of protein were size-separated by SDS-PAGE. The primary antibodies used in immunoblot analyses are listed in Supplementary Table S1. After incubation with the appropriate HRP-conjugated secondary antibodies (Santa Cruz Biotechnology), the immune reaction was developed by enhanced chemiluminescence (SuperSignal West Pico, Life Technologies, Milan, Italy). C-DiGit Blot Scanner (Lincoln, Nebraska, USA) was used for blot analysis.

Transfection assay. For NF-κB transcriptional activity, myoblasts in GM were transfected with NF-κB-luc reporter gene using jetPEI (Polyplus Transfections) as recommended by the manufacturer. After 24 h the cells were subjected to Firefly Luciferase Assay (Mirus, Madison, WI, USA) as recommended by the manufacturer. For transfection with bovine *S100b*, myoblasts in GM were transfected with pGMTSV-NEO S100B or empty vector for 24 h using jetPEI (Polyplus Transfections, New York, NY, USA) as recommended by the manufacturer. For siRNA transfection, myoblasts in GM were transfected with either S100B siRNA (Dharmacon, Carlo Erba Reagents Srl, Milan, Italy, ON-TARGET plus mouse S100B), YY1 siRNA (Gibco Life Technologies) or negative controls (Dharmacon, siRNA SMARTpoll control for S100B, and Invitrogen, Negative Universal Control Stealth for YY1) for 24 h using INTERFERin (Polyplus Transfections) as recommended by the manufacturer.

Real-time PCR. Total RNA was extracted from cell cultures using TRIsure (Bioline) according to the manufacturer's instructions and reverse-transcribed with M-MLV Reverse Transcriptase (Life Technologies, Milan, Italy). Real-time PCR analyses of mRNA contents were performed on Stratagene Mx3000P (Agilent Technologies, Santa Clara, CA, USA) by using HOT FIREPol EvaGreen qPCR Mix Plus (ROX) ready-to-use solution (Solis BioDyne, Tartu, Estonia) in the presence of the primer sets in Supplementary Table S2. *Gapdh* was used as an internal standard.

Animal treatment. C57BL/6 mice were obtained from Charles River. Primary myoblasts were isolated from 3-d-old WT (C57BL/6) pups and cultivated as described,[60] and characterized by immunofluorescence using a polyclonal anti-c-Met antibody (Santa Cruz Biotechnology) after fixation with cold methanol for 7 min at -20 °C. Greater than 95% cells were c-Met-positive. GC muscles were removed, fixed in 4% formalin in PBS (pH 7.2) and paraffin embedded for immunofluorescence analyses. Approval of use of animals was obtained by the Ethics Committee of the Perugia University and the Ministero della Salute, Italy. All methods were performed in accordance with the relevant guidelines and regulations of the Perugia University and the Ministero della Salute, Italy.

Immunofluorescence. Paraffin sections of GC muscles were cut at 4 μm, deparaffinized with xylene, rehydrated in a graded ethanol series. Antigen retrieval was obtained by boiling for 2 h in 10 mM citric acid buffer (pH 6.0), and depletion of endogenous peroxidase was accomplished by treatment with 3% H_2O_2 in methanol for 30 min. Sections were washed with PBS, pH 7.4, incubated for 1 h with blocking buffer (PBS containing 0.04% Triton X-100, 10% HS and 1% BSA) and then probed with mouse monoclonal anti-S100B antibody (R&D Systems, Minneapolis, MN, Toll Free USA, Canada) or rabbit polyclonal anti-UCP-1 antibody (Abcam ab10983). The antibodies were diluted (1:50) in 1% BSA in PBS and the sections incubated overnight in a humid chamber at 4 °C. After several washings with Tween-PBS, the sections were incubated with appropriate secondary fluorophore-antibodies (1:100 in 1% BSA in PBS; Gibco Life Technologies) for 2 h. The sections were then rinsed with Tween-PBS. Nuclei were counterstained with DAPI. After rinsing, samples were mounted with fluorescent mounting medium (Dako Corporation) and viewed in an epifluorescence microscope (Leica DMRB) equipped with a digital camera.

Statistical analysis. Each experiment was repeated at least three times. Representative experiments are shown unless stated otherwise. The data were subjected to analysis of variance with SNK *post hoc* analysis using a statistical software package (GraphPad Prism version 4.00, GraphPad Software, Inc., La Jolla, CA, USA). Data are the results of at least three independent experiments and are expressed as mean ± S.E.M.

Conflict of Interest

The authors declare no conflict of interest.

Acknowledgements. Ministero dell'Istruzione, dell'Università e della Ricerca, Italy (FIRB RBFR12BUMH) to IB and Ministero dell'Istruzione, dell'Università e della Ricerca, Italy (PRIN 2010R8JK2X_004) and Fondazione Cassa di Risparmio di Perugia (CRP 2016-0136.021) to RD.

1. Mitchell WK, Williams J, Atherton P, Larvin M, Lund J, Narici M. Sarcopenia, dynapenia, and the impact of advancing age on human skeletal muscle size and strength; a quantitative review. *Front Physiol* 2012; **3**: 260.
2. Cohen S, Nathan JA, Goldberg AL. Muscle wasting in disease: molecular mechanisms and promising therapies. *Nat Rev Drug Discov* 2015; **14**: 58–74.
3. Verdijk LB, Snijders T, Drost M, Delhaas T, Kadi F, van Loon LJ. Satellite cells in human skeletal muscle; from birth to old age. *Age (Dordr)* 2014; **36**: 545–547.
4. Dumont NA, Wang YX, Rudnicki MA. Intrinsic and extrinsic mechanisms regulating satellite cell function. *Development* 2015; **142**: 1572–1581.
5. Conboy IM, Conboy MJ, Wagers AJ, Girma ER, Weissman IL, Rando TA. Rejuvenation of aged progenitor cells by exposure to a young systemic environment. *Nature* 2005; **433**: 760–764.

6. Brack AS, Conboy MJ, Roy S, Lee M, Kuo CJ, Keller C *et al.* Increased Wnt signaling during aging alters muscle stem cell fate and increases fibrosis. *Science* 2007; **317**: 807–810.
7. Cosgrove BD, Gilbert PM, Porpiglia E, Mourkioti F, Lee SP, Corbel SY *et al.* Rejuvenation of the muscle stem cell population restores strength to injured aged muscles. *Nat Med* 2014; **20**: 255–264.
8. Bernet JD, Doles JD, Hall JK, Kelly Tanaka K, Carter TA, Olwin BB. p38 MAPK signaling underlies a cell-autonomous loss of stem cell self-renewal in skeletal muscle of aged mice. *Nat Med* 2014; **20**: 265–271.
9. Sousa-Victor P, Gutarra S, García-Prat L, Rodriguez-Ubreva J, Ortet L, Ruiz-Bonilla V *et al.* Geriatric muscle stem cells switch reversible quiescence into senescence. *Nature* 2014; **506**: 316–321.
10. Price FD, von Maltzahn J, Bentzinger CF, Dumont NA, Yin H, Chang NC *et al.* Inhibition of JAK-STAT signaling stimulates adult satellite cell function. *Nat Med* 2014; **20**: 1174–1181 Erratum in: *Nat Med* 2015; **21**:414. *Nat Med* 2014; Oct;(10): 1217.
11. García-Prat L, Martínez-Vicente M, Perdiguero E, Ortet L, Rodríguez-Ubreva J, Rebollo E *et al.* Autophagy maintains stemness by preventing senescence. *Nature* 2016; **529**: 37–42.
12. Marzetti E, Calvani R, Cesari M, Buford TW, Lorenzi M, Behnke BJ *et al.* Mitochondrial dysfunction and sarcopenia of aging: from signaling pathways to clinical trials. *Int J Biochem Cell Biol* 2013; **45**: 2288–2301.
13. Vasilaki A, Jackson MJ. Role of reactive oxygen species in the defective regeneration seen in aging muscle. *Free Radic Biol Med* 2013; **65**: 317–323.
14. Song MY, Ruts E, Kim J, Janumala I, Heymsfield S, Gallagher D. Sarcopenia and increased adipose tissue infiltration of muscle in elderly African American women. *Am J Clin Nutr* 2004; **79**: 874–880.
15. Solomon AM, Bouloux PM. Modifying muscle mass-the endocrine perspective. *J Endocrinol* 2006; **191**: 349–360.
16. Uezumi A, Fukada S, Yamamoto N, Takeda S, Tsuchida K. Mesenchymal progenitors distinct from satellite cells contribute to ectopic fat cell formation in skeletal muscle. *Nat Cell Biol* 2010; **12**: 143–152.
17. Joe AW, Yi L, Natarajan A, Le GF, So L, Wang J *et al.* Muscle injury activates resident fibro/adipogenic progenitors that facilitate myogenesis. *Nat Cell Biol* 2010; **12**: 153–163.
18. Saccone V, Consalvi S, Giordani L, Mozzetta C, Barozzi I, Sandoná M *et al.* HDAC-regulated myomiRs control BAF60 variant exchange and direct the functional phenotype of fibro-adipogenic progenitors in dystrophic muscles. *Genes Dev* 2014; **28**: 841–857.
19. Starkey JD, Yamamoto M, Yamamoto S, Goldhamer DJ. Skeletal muscle satellite cells are committed to myogenesis and do not spontaneously adopt nonmyogenic fates. *J Histochem Cytochem* 2011; **59**: 33–46.
20. Asakura A, Komaki M, Rudnicki M. Muscle satellite cells are multipotential stem cells that exhibit myogenic, osteogenic, and adipogenic differentiation. *Differentiation* 2001; **68**: 245–253.
21. Seale P, Asakura A, Rudnicki MA. The potential of muscle stem cells. *Dev Cell* 2001; **1**: 333–342.
22. Shefer G, Wleklinski-Lee M, Yablonka-Reuveni Z. Skeletal muscle satellite cells can spontaneously enter an alternative mesenchymal pathway. *J Cell Sci* 2004; **117**: 5393–5404.
23. Atashi F, Modarressi A, Pepper MS. The role of reactive oxygen species in mesenchymal stem cell adipogenic and osteogenic differentiation: a review. *Stem Cells Dev* 2015; **24**: 1150–1163.
24. Csete M, Walikonis J, Slawny N, Wei Y, Korsnes S, Doyle JC *et al.* Oxygen-mediated regulation of skeletal muscle satellite cell proliferation and adipogenesis in culture. *J Cell Physiol* 2001; **189**: 189–196.
25. Frühbeck G, Sesma P, Burrell MA. PRDM16: the interconvertible adipo-myocyte switch. *Trends Cell Biol* 2009; **19**: 141–146.
26. Seale P, Bjork B, Yang W, Kajimura S, Chin S, Kuang S *et al.* PRDM16 controls a brown fat/skeletal muscle switch. *Nature* 2008; **454**: 961–967.
27. Lepper C, Fan CM. Inducible lineage tracing of Pax7-descendant cells reveals embryonic origin of adult satellite cells. *Genesis* 2010; **48**: 424–436.
28. Seale P, Kajimura S, Yang W, Chin S, Rohas LM, Uldry M *et al.* Transcriptional control of brown fat determination by PRDM16. *Cell Metab* 2007; **6**: 38–54.
29. Tseng YH, Kokkotou E, Schulz TJ, Huang TL, Winnay JN, Taniguchi CM *et al.* New role of bone morphogenetic protein 7 in brown adipogenesis and energy expenditure. *Nature* 2008; **454**: 1000–1004.
30. Donato R, Sorci G, Riuzzi F, Arcuri C, Bianchi R, Brozzi F *et al.* S100B's double life: intracellular regulator and extracellular signal. *Biochim Biophys Acta* 2009; **1793**: 1008–1022.
31. Tubaro C, Arcuri C, Giambanco I, Donato R. S100B protein in myoblasts modulates myogenic differentiation via NF-κB-dependent inhibition of MyoD expression. *J Cell Physiol* 2010; **223**: 270–282.
32. Sorci G, Agneletti A, Donato R. Effects of S100A1 and S100B on microtubule stability. An in vitro study using triton-cytoskeletons from astrocyte and myoblast cell lines. *Neuroscience* 2000; **99**: 773–783.
33. Garbuglia M, Verzini M, Giambanco I, Spreca A, Donato R. Effects of calcium-binding proteins (S100ao, S100a, S100b) on desmin assembly in vitro. *FASEB J* 1996; **10**: 317–324.
34. Beccafico S, Riuzzi F, Puglielli C, Mancinelli R, Fulle S, Sorci G *et al.* Human muscle satellite cells show age-related differential expression of S100B protein and RAGE. *Age (Dordr)* 2011; **33**: 523–541.
35. Tubaro C, Arcuri C, Giambanco I, Donato R. S100B in myoblasts regulates the transition from activation to quiescence and from quiescence to activation, and reduces apoptosis. *Biochim Biophys Acta* 2011; **1813**: 1092–1104.
36. Cochemé HM, Murphy MP. Complex I is the major site of mitochondrial superoxide production by paraquat. *J Biol Chem* 2008; **283**: 1786–1798.
37. Akiyama K, Tone J, Okabe M, Nishimoto S, Sugahara T, Kakinuma Y. Inhibition of myotube formation by paraquat in the myoblast cell line C2C12. *J Toxicol Sci* 2011; **36**: 243–246.
38. Chargé SB, Rudnicki MA. Cellular and molecular regulation of muscle regeneration. *Physiol Rev* 2004; **84**: 209–238.
39. Mendelson KG, Contois LR, Tevosian SG, Davis RJ, Paulson KE. Independent regulation of JNK/p38 mitogen-activated protein kinases by metabolic oxidative stress in the liver. *Proc Natl Acad Sci USA* 1996; **93**: 12908–12913.
40. Zhou LZ, Johnson AP, Rando TA. NF kappa B and AP-1 mediate transcriptional responses to oxidative stress in skeletal muscle cells. *Free Radic Biol Med* 2001; **31**: 1405–1416.
41. Sorci G, Giovannini G, Riuzzi F, Bonifazi P, Zelante T, Zagarella S *et al.* The danger signal S100B integrates pathogen- and danger-sensing pathways to restrain inflammation. *PLoS Pathog* 2011; **7**: e1001315.
42. Wang H, Hertlein E, Bakkar N, Sun H, Acharyya S, Wang J *et al.* NF-κB regulation of YY1 inhibits skeletal myogenesis through transcriptional silencing of myofibrillar genes. *Mol Cell Biol* 2007; **27**: 4374–4387.
43. Zhang D, Li X, Chen C, Li Y, Zhao L, Jing Y *et al.* Attenuation of p38-mediated miR-1/133 expression facilitates myoblast proliferation during the early stage of muscle regeneration. *PLoS ONE* 2012; **7**: e41478.
44. Feng Y, Niu LL, Wei W, Zhang WY, Li XY, Cao JH *et al.* A feedback circuit between miR-133 and the ERK1/2 pathway involving an exquisite mechanism for regulating myoblast proliferation and differentiation. *Cell Death Dis* 2013; **4**: e934.
45. Trajkovski M, Ahmed K, Esau CC, Stoffel M. MyomiR-133 regulates brown fat differentiation through Prdm16. *Nat Cell Biol* 2012; **14**: 1330–1335.
46. Yin H, Pasut A, Soleimani VD, Bentzinger CF, Antoun G, Thorn S *et al.* MicroRNA-133 controls brown adipose determination in skeletal muscle satellite cells by targeting *Prdm16*. *Cell Metab* 2013; **17**: 210–224.
47. Lu L, Zhou L, Chen EZ, Sun K, Jiang P, Wang L *et al.* 2012 A novel YY1-miR-133 regulatory circuit in skeletal myogenesis revealed by genome-wide prediction of YY1-miRNA network. *PLoS ONE* 2012; **7**: e27596.
48. Fulle S, Di Donna S, Puglielli C, Pietrangelo T, Beccafico S, Bellomo R *et al.* Age-dependent imbalance of the antioxidative system in human satellite cells. *Exp Gerontol* 2005; **40**: 189–197.
49. Student AK, Hsu RY, Lane MD. Induction of fatty acid synthetase synthesis in differentiating 3T3-L1 preadipocytes. *J Biol Chem* 1980; **255**: 4745–4750.
50. Mancini A, El Bounkari O, Norrenbrock AF, Scherr M, Schaefer D, Eder M *et al.* FMIP controls the adipocyte lineage commitment of C2C12 cells by downmodulation of c/EBPα. *Oncogene* 2007; **26**: 1020–1027.
51. Endo T, Kusakabe M, Sunadome K, Yamamoto T, Nishida E. The kinase SGK1 in the endoderm and mesoderm promotes ectodermal survival by down-regulating components of the death-inducing signaling complex. *Sci Signal* 2011; **4**: ra2.
52. Blättler SM, Verdeguer F, Liesa M, Cunningham JT, Vogel RO, Chim H *et al.* Defective mitochondrial morphology and bioenergetic function in mice lacking the transcription factor Yin Yang 1 in skeletal muscle. *Mol Cell Biol* 2012; **32**: 3333–3346.
53. Verdeguer F, Soustek MS, Hatting M, Blättler SM, McDonald D, Barrow JJ *et al.* Brown adipose YY1 deficiency activates expression of secreted proteins linked to energy expenditure and prevents diet-induced obesity. *Mol Cell Biol* 2015; **36**: 184–196.
54. Han Y, Choi YH, Lee SH, Jin YH, Cheong H, Lee KY. Yin Yang 1 is a multi-functional regulator of adipocyte differentiation in 3T3-L1 cells. *Mol Cell Endocrinol* 2015; **413**: 217–227.
55. Michetti F, Dell'Anna E, Tiberio G, Cocchia D. Immunochemical and immunocytochemical study of S-100 protein in rat adipocytes. *Brain Res* 1983; **262**: 352–356.
56. Barbatelli G, Morroni M, Vinesi P, Cinti S, Michetti F. S-100 protein in rat brown adipose tissue under different functional conditions: a morphological, immunocytochemical, and immunochemical study. *Exp Cell Res* 1993; **208**: 226–231.
57. Kapucuoglu N, Percinel S, Angelone A. Adenohibernoma of the breast. *Virchows Arch* 2008; **452**: 351–352.
58. Di Tommaso L, Chiesa G, Arena V, Guanella G, Galli C, Roncalli M. Cardiac hibernoma: a case report. *Histopathology* 2012; **61**: 985–987.
59. Vlychou M, Teh J, Whitwell D, Athanasou NA. Intraosseous hibernoma: a rare adipocytic bone tumour. *Skeletal Radiol* 2016; **45**: 1565–1569.
60. Neville C, Rosenthal N, McGrew M, Tsakiris T, Parthimos N, Hauschka S. (1997) Skeletal muscle cultures. *Methods Cell Biol* 1997; **52**: 85–116.

Supplementary Information accompanies this paper on Cell Death and Differentiation website (http://www.nature.com/cdd)